Krasheninnikov, A. V.; Lehtinen, P.O.; Foster, A. S.; Pyykkö, P.; Nieminen, R. M.

Embedding transition-metal atoms in graphene: Structure, bonding, and magnetism

Published in:
Physical Review Letters

DOI:
10.1103/PhysRevLett.102.126807

Published: 01/01/2009

Document Version
Publisher's PDF, also known as Version of record

Please cite the original version:
Krasheninnikov, A. V., Lehtinen, P. O., Foster, A. S., Pyykkö, P., & Nieminen, R. M. (2009). Embedding transition-metal atoms in graphene: Structure, bonding, and magnetism. *Physical Review Letters*, *102*(12), 1-4. Article 126807. https://doi.org/10.1103/PhysRevLett.102.126807

Embedding Transition-Metal Atoms in Graphene: Structure, Bonding, and Magnetism

A. V. Krasheninnikov,[1,2,*] P. O. Lehtinen,[1] A. S. Foster,[1,3] P. Pyykkö,[4] and R. M. Nieminen[1]

[1]*Laboratory of Physics, Helsinki University of Technology, P.O. Box 1100, FI-02015, Finland*
[2]*Materials Physics Division, University of Helsinki, P.O. Box 43, FI-00014, Finland*
[3]*Department of Physics, Tampere University of Technology, P.O. Box 692, 33101 Tampere, Finland*
[4]*Department of Chemistry, University of Helsinki, P.O. Box 55, FI-00014, Finland*

(Received 8 January 2009; published 26 March 2009)

We present a density-functional-theory study of transition-metal atoms (Sc–Zn, Pt, and Au) embedded in single and double vacancies (SV and DV) in a graphene sheet. We show that for most metals, the bonding is strong and the metal-vacancy complexes exhibit interesting magnetic behavior. In particular, an Fe atom on a SV is not magnetic, while the Fe@DV complex has a high magnetic moment. Surprisingly, Au and Cu atoms at SV are magnetic. Both bond strengths and magnetic moments can be understood within a simple local-orbital picture, involving carbon sp^2 hybrids and the metal spd orbitals. We further calculate the barriers for impurity-atom migration, and they agree well with available experimental data. We discuss the experimental realization of such systems in the context of spintronics and nanocatalysis.

DOI: 10.1103/PhysRevLett.102.126807 PACS numbers: 73.22.−f, 61.48.De, 61.72.Bb, 75.20.Hr

A considerable body of experimental work [1] has confirmed the theoretical predictions [2] that the linear dispersion of two-dimensional massless quasiparticles in graphene [3] can give rise to unusual physics. One case which has been widely discussed in the context of spintronics and unconventional Kondo physics is the effect of impurities on the local electronic and magnetic structure of a single graphene sheet [4–7].

Nearly all theoretical work [4–6] on the Kondo effect in graphene has been based on model Hamiltonians, not taking into account the actual electronic structure of the graphene sheet with impurities. Moreover, in spite of several suggestions for experimental realization of Kondo systems in graphene [5], e.g., by substitution of carbon with transition-metal (TM) atoms, the stability of such structures and their magnetic properties have not been studied. It is not even clear if substitutional TM atoms in the graphene sheet have magnetic moments. In general, simplistic assumptions about TM behavior are rarely valid, as their properties can vary widely in various hosts [8]. Furthermore, the precise knowledge of the TM–sp^2-carbon interaction is important for understanding carbon nanotube growth [9], fuel cell properties [10], and the role of implanted magnetic atoms such as Fe in the development of magnetic order in carbon materials [11].

Here we present a systematic first-principles study of the TM atom impurities in graphene. In order to provide a comprehensive comparison, we studied all TM atoms from Sc to Zn. We further included Au and Pt, as their interaction with a single graphene sheet has recently been investigated experimentally in a transmission electron microscope (TEM) [12], with an aim to link our results to the known experimental data on the atom positions in graphene sheet and their diffusivities. We calculate the atomic structure of TM atoms adsorbed on pristine and defected graphene, containing single and double vacancies (SV and DV), and study the stability of various defect configurations by comparing their relative energies and evaluating migration barriers. We show that nearly all TM atoms strongly bind to the defected graphene, and that the hybridization of carbon sp^2 and metal spd orbitals, combined with a different environment of the atom at SVs and DVs, gives rise to very peculiar magnetic properties of the atom-vacancy complexes.

We used the spin-polarized density-functional theory (DFT) as implemented in the plane-wave-basis-set VASP [13] code. We used projector augmented wave (PAW) potentials [14] to describe the core electrons and the generalized gradient approximation of Perdew, Burke, and Ernzernhof (PBE) [15] for exchange and correlation. A kinetic energy cutoff of 400 eV was used in most simulations. Increasing the cutoff energy up to 700 eV changed the bonding energies by less than 10 meV, as checked for Fe, Co, Ni, Au, and Pt. The same accuracy was also achieved with respect to the $\mathbf{k}$-point sampling over the Brillouin zone (with meshes up to 19×19 $\mathbf{k}$-points). This approach has been demonstrated to be adequate for the modeling of defects in graphitic systems [16] and TM impurities in various matrices [8,17].

All simulations were carried out for a 98-atom graphene supercell (7×7 graphene unit cells), approaching the single impurity limit (impurity concentration of about 1%). Several test calculations for a 200-atom (10×10 unit cells) and a rectangular 112-atom supercells gave essentially the same results. The total spin was not fixed during the structure relaxation, and the Fermi smearing (with a width of 0.1 eV) of the electronic levels was used. Lower values of smearing (0.02 eV) were used to get the accurate spin configurations for the relaxed structures. The climbing-image nudged-elastic-band method [18] was used for calculating the migration barriers.

Bearing in mind possible implementations of Kondo systems by metal atom chemisorption on graphene [5], we first studied the behavior of TM atoms adsorbed on perfect graphene sheets. In agreement with the previous calculations [17,19], we found that the TM adatoms on pristine graphene had binding energies of 0.2–1.5 eV. We also calculated the migration barriers for adatoms. The barriers proved to be low, in the range of 0.2–0.8 eV, which indicates that the adatoms should be mobile at room temperature. Although some adatoms do have magnetic moments, the controlled chemisorption of metal atoms on pristine graphene can hardly be used for manufacturing graphene-based Kondo systems, as very low temperatures would be required to prevent atom motion. Besides, even at low temperatures the deposition of the adatom with atomic accuracy is very difficult to achieve.

We now turn to metal atoms adsorbed on SVs in a graphene sheet. Such a structure can be associated with a substitutional impurity in graphene. We found that all metal atoms considered, including Au, form covalent bonds with the under-coordinated C atoms at the vacancy by breaking the weak C—C bond (bond length 2.04 Å) at the pentagon in the reconstructed vacancy [16,20]. The typical atomic configuration of a M@SV complex is shown in Fig. 1. As the TM atomic radii are larger than that of the carbon atom, the metal atoms displace outwards from the graphene surface, as reported earlier for Ni [21], although the elevation h is considerably lower (by nearly 1 Å) than for the adatoms. The binding energies E_b, calculated as a difference between the metal atom in the substitutional position and the energy of a reconstructed naked vacancy [16,20] plus energy of the isolated atom, are presented in Fig. 2(b). The typical values of E_b are about -7 eV [22], except for the atoms with almost full d-shells, such as Cu and Zn. Pt atoms also bind strongly to SV, as reported previously for carbon nanotubes [23]. The

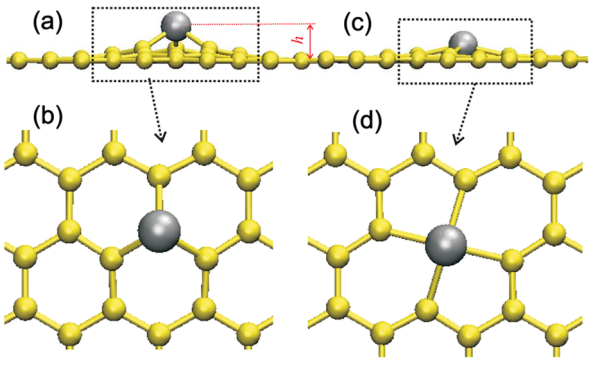

FIG. 1 (color online). Typical atomic configurations of TM atoms adsorbed on single and double vacancies in a graphene sheet. Metal atom on a single vacancy: Side view (a), top view (b). Note that the metal atom is above the surface, with an elevation h of up to 2 Å. Metal atom on a double vacancy: Side view (c) and top view (d). The grey balls are metal atoms, the yellow balls carbon atoms. The structure of a V@DV complex is shown in the inset in Fig. 2.

TM—C bond length decreases from Sc to Fe as the atom size decreases, Fig. 3(a), then it goes up as the bonding becomes weaker. It lies between the sum of the most recent predictions of triple and single-bond covalent radii [24], except Au-C, which is longer.

We found that the M@SV complexes are magnetic for M = V, Cr, and Mn, which have single-filled d states. The Fe and Ni impurities having double occupied states and an even number of electrons are nonmagnetic, while Co and Cu, having an odd number of electrons, are magnetic.

The behavior of M@DV complexes is even more interesting. While Sc and Ti atoms form the "cross" configuration shown in Fig. 1(c), V is two coordinated with a configuration corresponding to the naked DV in graphene [20]. The M@DV complexes are magnetic for all TM from V to Co. Prior to discussing the details of the electronic structures of these complexes, one can note that these results are consistent with the general crystal field theory: A larger "hole" at the DV should result in a weaker interaction of the impurity atom with the ligand bonds, and thus in higher spin states of the complex.

In order to understand the reason for such a behavior we calculated the band structures (BS) of the graphene-impurity system. The BS of a Mn@DV complex, typical for other TM with single-filled d states, is shown in Fig. 4(a). A number of strongly hybridized states of metal-carbon bonding character with a small dispersion appear close to the Fermi energy E_F and below (down to -7 eV). These states give rise to sharp peaks in the spin-polarized density of states (SP-DOS), Fig. 4(b). The energy-resolved magnetization densities associated with these metal-induced states (energy intervals from 0 to -0.2; -0.2 to -0.4; -1 to -1.6; -1.6 to -4 eV) are presented in

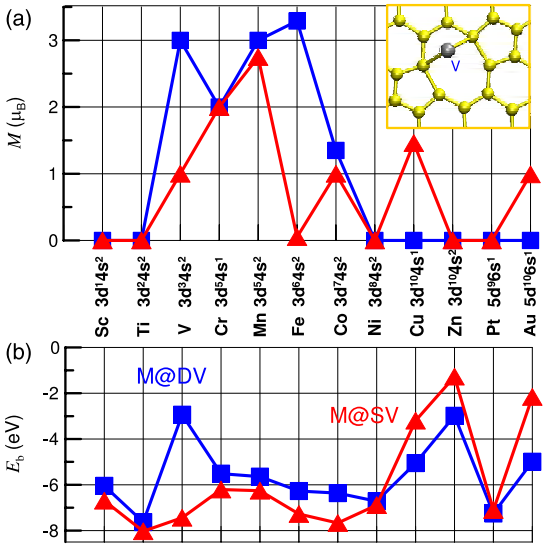

FIG. 2 (color online). Magnetic moments, M (a) and binding energies, E_b (b) of the graphene sheet with TM atoms adsorbed on SVs and DVs (red and blue curves, respectively). The inset shows the configuration for V atom on DV which is different from those for all other atoms. The lines guide the eye.

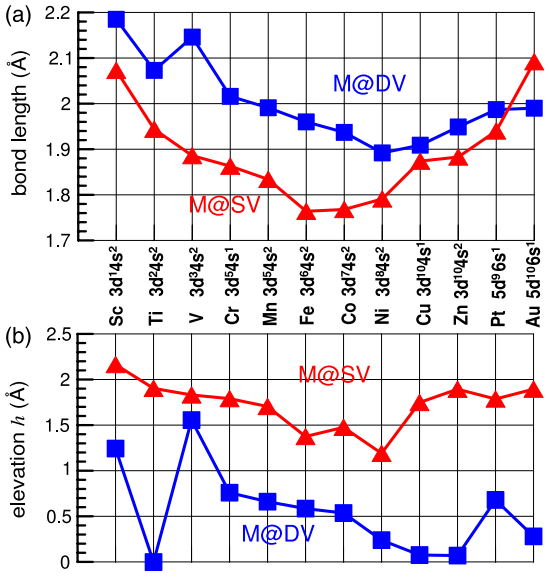

FIG. 3 (color online). Metal-carbon bond lengths (a) and elevation (b) of the metal atom above the graphene surface of TM atoms, adsorbed on SVs and DVs in a graphene sheet.

Figs. 4(d)–4(g), respectively. The total magnetic moments of the system corresponding to these energy ranges are 0.6, 0.5, -0.7, and 2.6 μ_B, respectively. The moments of the states, associated with strongly hybridized carbon bonds, partly compensate each other. Hence the contribution of the more localized nonbonding d-orbitals determines the spin configuration. The analysis of energy-resolved magnetization densities for other TM atoms at SVs and DVs showed that the total magnetic moment of the system comes mostly from the metal atom (local moments of 1, 2, 3, and 1μ_B for V, Cr, Mn, and Co, respectively) and partly from its neighbors, as shown in Figs. 4(c) and 4(h) through the example of Mn.

By comparing the BS of the impurity complexes to those of pristine and defected graphene sheets, we developed a simple model, which can qualitatively explain the trends in bonding and magnetic properties. It is instructive to start the analysis with the Ti@SV complex. The Ti atom has four valence electrons. One can assume that three of them go into the Ti—C covalent σ bonds depicted with double dots in Fig. 4(i), while the fourth (depicted as the circle) replaces the π electron of the missing carbon atom. This yields three σ bonds and one (slightly out-of-plane) π bond. Four valencies are saturated and the spin is zero. In other words, the tetravalent Ti atom is a perfect substitution for a tetravalent C atom, and it binds strongly. In this case, the E_b is the largest among all TM atoms. Sc has to import one π electron and $M = 0$. V, Cr, and Mn have 1, 2 and 3 extra electrons, respectively, which go to separate nonbonding orbitals [red arrows in Fig. 4(i)] and give rise to $M = 1, 2$, and $3\mu_B$. Note that a d element (such as Ti or Pt) has in total nine localized spd orbitals [25]. The situation changes when the TM atom has more than 5 electrons so that some of the nonbonding orbitals are filled. The Coulomb interaction gives rise to a shift of the impurity states into the conduction band or/and opening of a minigap at E_F [26]. At Fe@SV the spins pair up to $M = 0$, as for Ni@SV, and its homolog Pt@SV. The atoms with an odd number of electrons (Co, Cu, and its Group-11 homolog Au) still have a unitary magnetic moment.

Similar ideas can be applied to M@DV complexes. Now there are four local σ bonds [Fig. 4(j)], and one potential local π bond. However, the π M—C interaction is weaker, due to a larger separation between the metal and carbon atoms. Besides, the π electrons on the dangling bond

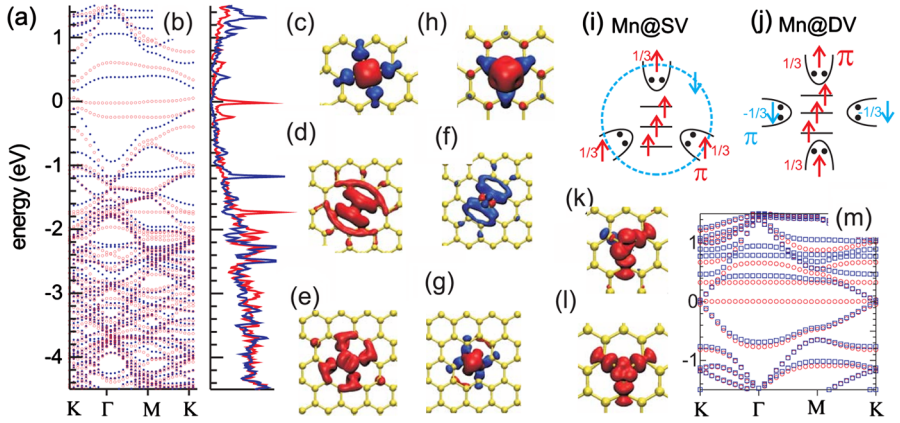

FIG. 4 (color online). Typical electronic structures of metal atoms at SVs and DVs. Band structure (a) and spin-polarized density of states (b) of a Mn@DV complex. Red (blue) symbols correspond to the majority (minority) spin. Zero energy corresponds to the Fermi energy. Isosurface of the total (c) and energy-resolved (d)–(g) magnetization density for the Mn@DV complex. Energy intervals are: 0 to -0.2 eV (d); -0.2 to -0.4 eV (e); -1 to -1.6 eV (f); -1.6 to -4 eV (g). Red color corresponds to positive values of the spin density, blue to the negative values. (h) Magnetization density for the Mn@SV complex. Schematic representations of the electronic structure of a Mn@SV (i) and Mn@DV (j) complexes. Here the numbers "1/3" symbolically represent the ligand contribution to the approximate π bond, as one π electron is shared among three π-bonds. Magnetization density for the Au@SV (k) and Cu@SV (l) complexes and band structure (m) for the Au@SV complex.

atoms in a naked DV have opposite spins, as they are on different sublattices, which increases direct interaction between the dangling bond C atoms.

The cross configuration for Ti shown in Fig. 1 is absolutely flat and it is not magnetic. In case of the V@DV complex, it is energetically favorable for the system to reconstruct as in the case of a naked DV [20], so that the V atom becomes a double-coordinated adatom. Three nonbonded electrons of the V atom give rise to a magnetic moment of $3\mu_B$, Fig. 2(a). For Co and Mn (with cross configurations), the magnetic moment is 2 and $3\mu_B$, in agreement with the simple counting rules. One can expect that the magnetic moment should go down for metals after Mn. This trend is correct, apart from Fe: the total magnetic moment of the system is over three. The analysis of magnetization on atoms indicated that at least $0.5\mu_B$ comes from the neighboring C atoms. The cross configurations for Cu, Zn, and Au are nonmagnetic and essentially flat, Fig. 3(b).

The magnetism for the Cu and Au@SV complexes is somewhat different from the case of other TM atoms. As Cu and Au have filled d shells, a considerable part of the atom magnetization comes from the s and p states (50% for Au and 30% for Cu). Moreover, about half of the total magnetization is due to the neighboring C atoms, Figs. 4(k) and 4(l). The spin-polarized states appear just at E_F, Fig. 4(m).

To assess the stability of M@SV and M@DV complexes, we also studied the energetics and migration of metal atoms in various configurations. We found that although it is energetically favorable for all metal atoms to form a cluster at a defect site, the migration barriers for M@SV complexes are relatively high. The M@SV complexes migrate by rotating one of the metal-carbon bonds with an activation barrier of 2.1, 3.1, 3.6, 3.2, and 3.1 eV for Au, Pt, Fe, Co, and Ni, respectively. The former two values are in a reasonable agreement with the experimental data of 2.4 and 2.6 eV, respectively [12]. One can expect that the migration barriers for other TM atoms should be of the same order, so that the M@SV complexes would not move at room temperature, contrary to the adatoms on the surface of pristine graphene. The activation barriers for M@DV complexes proved to be about 5 eV, in agreement with recent theoretical results for Au [27].

The high mobility of metal adatoms and low mobility of M@SV and DV complexes can be used for engineering the position of metal atoms with atomic precision. Graphene flakes with small metal clusters or adatoms can be created by coevaporation [12], then deposited on a TEM grid. Using the TEM with a focused (down to 1 Å in diameter) electron beam [28], one can displace C atoms with atomic precision and create an array of vacancies. Then the temperature can be raised, so that the TM adatoms become mobile unless they are pinned by the vacancies. The experimental implementation of such systems, which should be extremely interesting for spintronics, is underway [29]. At the same time, large-scale ion irradiation of coevaporated metal-carbon systems may be used for developing metal-graphene materials for catalysis.

We thank F. Banhart, A. Ayuela, D. Sánchez-Portal, and C. Ewels for useful discussions. This work was supported by The Academy of Finland Centres of Excellence CMS and COMP. The Finnish IT Center for Science provided generous grants of computer time.

*akrashen@acclab.helsinki.fi

[1] A. K. Geim and K. S. Novoselov, Nature Mater. **6**, 183 (2007).
[2] A. H. Castro Neto *et al.*, Rev. Mod. Phys. **81**, 109 (2009).
[3] K. S. Novoselov *et al.*, Nature (London) **438**, 197 (2005).
[4] M. Hentschel and F. Guinea, Phys. Rev. B **76**, 115407 (2007).
[5] K. Sengupta and G. Baskaran, Phys. Rev. B **77**, 045417 (2008).
[6] B. Dóra and P. Thalmeier, Phys. Rev. B **76**, 115435 (2007).
[7] A. V. Shytov, M. I. Katsnelson, and L. S. Levitov, Phys. Rev. Lett. **99**, 236801 (2007).
[8] H. Raebiger, S. Lany, and A. Zunger, Nature (London) **453**, 763 (2008).
[9] O. V. Yazyev and A. Pasquarello, Phys. Rev. Lett. **100**, 156102 (2008).
[10] G. Che *et al.*, Nature (London) **393**, 346 (1998).
[11] R. Sielemann *et al.*, Phys. Rev. Lett. **101**, 137206 (2008).
[12] Y. Gan, L. Sun, and F. Banhart, Small **4**, 587 (2008).
[13] G. Kresse and J. Furthmüller, Comput. Mater. Sci. **6**, 15 (1996).
[14] P. E. Blöchl, Phys. Rev. B **50**, 17 953 (1994).
[15] J. P. Perdew, K. Burke, and M. Ernzerhof, Phys. Rev. Lett. **77**, 3865 (1996).
[16] P. O. Lehtinen *et al.*, Phys. Rev. Lett. **93**, 187202 (2004).
[17] H. Sevincli *et al.*, Phys. Rev. B **77**, 195434 (2008).
[18] G. Henkelman, B. P. Uberuaga, and H. Jónsson, J. Chem. Phys. **113**, 9901 (2000).
[19] K. T. Chan, J. B. Neaton, and M. L. Cohen, Phys. Rev. B **77**, 235430 (2008).
[20] A. A. El-Barbary *et al.*, Phys. Rev. B **68**, 144107 (2003).
[21] F. Banhart, J. C. Charlier, and P. M. Ajayan, Phys. Rev. Lett. **84**, 686 (2000).
[22] Note that binding energy of a C atom to graphene sheet with a single vacancy is about −14 eV.
[23] Y. Park, G. Kim, and Y. Hee Lee, Appl. Phys. Lett. **92**, 083108 (2008).
[24] P. Pyykkö, S. Riedel, and M. Patzschke, Chem. Eur. J. **11**, 3511 (2005); P. Pyykkö and M. Atsumi, Chem. Eur. J. **15**, 186 (2009).
[25] M. Patzschke and P. Pyykkö, Chem. Commun. (Cambridge) 17 (2004) 1982.
[26] E. J. G. Santos *et al.*, Phys. Rev. B **78**, 195420 (2008).
[27] S. Malola, H. Häkkinen, and P. Koskinen, Appl. Phys. Lett. **94**, 043106 (2009).
[28] A. V. Krasheninnikov and F. Banhart, Nature Mater. **6**, 723 (2007).
[29] F. Banhart (private communication).